JOURNAL OF CATALYSIS **160,** 214–221 (1996)
ARTICLE NO. 0140

Comparison of Silica-Supported MoO_3 and V_2O_5 Catalysts in the Selective Partial Oxidation of Methane

Marisol Faraldos,* Miguel A. Bañares,* James A. Anderson,† Hangchun Hu,‡ Israel E. Wachs,‡ and José Luís G. Fierro*

*Instituto de Catálisis y Petroleoquímica, C.S.I.C., UAM Cantoblanco, 28049 Madrid, Spain; †Department of Chemistry, The University, Dundee DD1 4HN, Scotland, United Kingdom; and ‡Zettlemoyer Center for Surface Studies and Department of Chemical Engineering, Lehigh University, Bethlehem, Pennsylvania 18015

Received April 19, 1995; revised October 26, 1995; accepted January 22, 1996

Silica-supported molybdenum oxide and vanadium oxide catalysts have been prepared with a wide range of surface metal loadings (0.3–3.5 metal atom/nm^2). Isolated surface metal oxide species are dominant at surface metal loadings on silica below ca. 1 metal atom/nm^2 while at higher loadings, the metal oxide species tend to aggregate into crystalline MoO_3 and V_2O_5 particles. Both catalyst series have been tested in the selective oxidation of methane with molecular oxygen at atmospheric pressure. The reactivity for methane conversion appears to be essentially related to dispersed isolated surface metal oxide species, with the surface vanadium oxide species being more reactive than molybdenum oxide species. The higher reactivity of the surface vanadium oxide sites may be related to the different nature of the interaction of the oxides with oxygen. Silica-supported vanadium oxide catalysts, despite their higher activity, result in lower yields to HCHO than silica-supported molybdenum oxide catalysts.

INTRODUCTION

The direct conversion of methane to formaldehyde and methanol in a single catalytic step in sufficiently high yield would give rise to new opportunities in the conversion of natural gas to other useful fuels and chemicals. Both the homogeneous and heterogeneous processes have been studied under various conditions (1–3) although progress toward obtaining a yield that would make such a process industrially viable has been very slow. The majority of these studies have involved metal oxide catalysts (4–24). In these studies, the CH_4/oxidant stoichiometry has been varied (20 to 0.5), with the temperature normally within the range 723–923 K as a result of the extremely low reaction rate at low temperatures, while above 900 K CO_x formation becomes much more dominant. High selectivities to methanol and formaldehyde (ca. 90%) at low methane conversion have been reported in the reaction with oxygen or nitrous oxide, although the selectivity drops drastically at increasing conversion leading to few reports of yields higher than ca. 2%. These limited yields arise from the unfavorable ratio of the reactivity of methane to formaldehyde and methanol.

Studies by Spencer and Pereira (8, 9) in the selective oxidation of methane over redox-type (MoO_3 and V_2O_5) catalysts indicate that the majority of carbon oxides are formed as a result of the deep oxidation of formaldehyde ($CH_4 \rightarrow HCHO \rightarrow CO_x$). The rate constant for the HCHO oxidation to CO derived from their data is 50–100 times higher than the rate constant for methane conversion. In line with the above argument, several authors have questioned the heterogeneous nature of the CH_4 oxidation. Baldwin *et al.* (16) raised serious doubts of the necessity to use a catalyst since the HCHO yield obtained from the heterogeneous process is still lower than that obtained from the homogeneous reaction. Hargreaves *et al.* (25) claimed a high yield to HCHO at 1023 K on MgO at very low oxygen conversion, but were unable to distinguish whether the oxidation of $CH_3\cdot$ radicals to HCHO occurred in the gas phase or on the surface.

The selection of appropriate experimental conditions as well as a precise reactor design, which minimizes the combustion or gas-phase reaction, would appear critical in obtaining reliable data. Using this approach, CH_4 oxidation on silica-supported molybdenum oxide was studied, and results indicate that the activity depends markedly on the MoO_3 content (26, 27). As one of the major issues in a partial oxidation reaction over oxide catalysts is the role of the lattice oxygen, a tracer $^{18}O_2$ isotopic technique was used for studying the mechanism of oxygen incorporation into CH_4 (22, 23, 28, 29). The results confirmed that the selective oxidation proceeds via a Mars–van Krevelen mechanism in which the lattice oxygen is incorporated into the formaldehyde molecule while the consumed oxygen is restored by dioxygen from gas phase (22, 23, 28, 29). The same applies to silica-supported vanadia catalysts although the binding energy of lattice oxygen is lower in V_2O_5 than in MoO_3 (30).

This present study was aimed at evaluating the activity of CH_4 partial oxidation on silica-supported MoO_3 and V_2O_5

0021-9517/96 $18.00

catalysts and attempting to relate catalytic performance with surface characteristics of the supported oxide phases.

EXPERIMENTAL

Catalyst Preparation

A commercial silica (Aerosil 200), particle size 12 nm, BET area 200 m^2/g, and composition $SiO_2 > 99.8\%$, $Al_2O_3 < 0.05\%$, $Fe_2O_3 < 0.003\%$, and $TiO_2 < 0.03\%$, was used as support. This was impregnated with an aqueous solution of ammonium metavanadate (NH_4VO_3, Merck reagent grade) with H_2O_2 or ammonium heptamolybdate ($(NH_4)_6Mo_7O_{24} \cdot 6H_2O$, Merck reagent grade) in appropriate amounts to give surface concentrations in the range 0.3–3.0 V or 0.3–3.5 Mo atoms/nm^2 of the silica surface assuming that all of the supported metal oxide is 100% dispersed. They are referred to as xV (or xMo), where x indicates the surface concentration in V (or Mo) atoms/nm^2 of the support. The impregnated silicas were dried at 383 K and calcined in two steps: 623 K for 2 h and 923 K for 5 h. Prior to use in the reaction the catalysts were pelleted and sieved within the particle size range 0.42–0.50 mm.

Methods

The reducibility and the initial rate of reduction of the catalysts were obtained from reduction isotherms performed at 823 K using a Cahn 2000 microbalance operating at a sensitivity of 10 μg. Catalyst samples were first heated at 4 K/min to 823 K in a flow (60 cm^3/min) of helium (99.997% vol) before measuring the kinetic reduction curves in a flow (60 cm^3/min) of H_2 (99.995% vol) at the same temperature. Weight changes as a function of time were collected by microprocessor and then differentiated at zero time thus allowing calculation of the initial rate of reduction.

Raman spectra of the dehydrated samples were measured using the 514.5 nm argon ion excitation line at a maximum power of 70 mW. The scattered radiation was passed through a Spex Triplemate spectrometer coupled to a multichannel analyzer with an intensified photodiode array cooled at 233 K. The overall resolution was better than 2 cm^{-1}. A pressed wafer was placed into a stationary sample holder located in an *in situ* cell (31, 32). Spectra were recorded in flowing oxygen at room temperature after the samples were dehydrated in flowing oxygen at 573 K.

Activity measurements were carried out at atmospheric pressure in a fixed-bed quartz microcatalytic reactor (8 mm o.d.) by co-feeding CH_4 (99.95% vol) and O_2 (99.98% vol) without diluent. The $CH_4 : O_2$ ratio was adjusted in the range 3–10 M by means of mass flow controllers and the methane residence time was adjusted to 0.4 or 2 g h/mol for vanadia and to 1.5 or 4.5 g h/mol for molybdena catalysts. The reactor effluent were analyzed by an on-line Konik 3000HR gas chromatograph fitted with a thermal conductivity detector. Chromosorb 107 and Molecular Sieve 5A packed columns were used with a column isolation analysis system.

RESULTS AND DISCUSSION

Structure of the Supported Oxides

Raman spectra of the dehydrated samples were recorded. Although water is generated under reaction conditions, which may influence the surface species resulting in changes in the Raman spectra of supported oxides, spectra obtained during methane oxidation conditions closely resemble spectra of dehydrated samples (33). Therefore, it is justifiable to compare spectra of dehydrated samples in order to distinguish between samples of different loadings. In the case of MoO_3/SiO_2 catalysts, a band at ca. 982 cm^{-1} is detected which is not present for silica alone. This band is due to the vibration mode of the terminal Mo=O bond of isolated distorted octahedral mono-oxo-molybdenum oxide species. At higher loadings a broadening of the Raman band toward lower wavenumber is observed, and a band appears at ca. 368 cm^{-1} due to the bending mode of the Mo=O. For 1.3Mo these features become broad Raman bands at ca. 968, 871, and 368 cm^{-1}, suggesting the presence of surface polymolybdate species in the dehydrated catalyst at molybdenum loadings close to the dispersion limit. For higher molybdenum loadings, Raman bands at 993, 817, 660, 284, 158, 129, and 117 cm^{-1} due to crystalline orthorhombic molybdenum oxide were observed.

Silica-supported vanadium oxide catalysts showed a Raman band at ca. 1035 cm^{-1}, characteristic of the stretching mode of the terminal bond V=O of isolated surface mono-oxo-vanadium oxide species with C_{3v} symmetry (34). A weak interaction between surface vanadium species is indicated by additional Raman bands at ca. 284 and 404 cm^{-1}, which are more apparent at higher vanadium loadings. Aggregation of vanadium oxide species is indicated by Raman features at 993, 702, 404, and 284 cm^{-1}, characteristic of crystalline V_2O_5 (34). Since the Raman bands of crystalline species are much more intense than those of dispersed surface species (32), the size and number of these crystals need not necessarily be high.

As the catalytic reaction involves the consumption of surface oxygen species, isothermal reduction experiments were performed at 823 K (within the range of reaction temperatures studied) and both the initial rate of reduction and overall reducibility were calculated. Experiments were conducted after no appreciable weight loss was observed in flowing helium at 823 K, thus ensuring that the silica-supported metal oxides were dehydrated prior to reduction measurements. For the silica-supported vanadium oxide catalysts, weight loss occurred during the first few minutes of reduction and stabilized after approximately 2 h. This

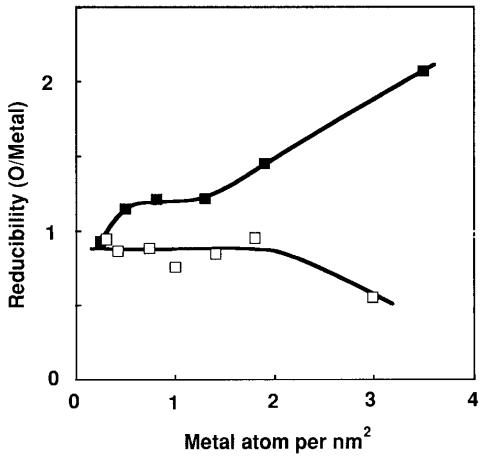

FIG. 1. Reducibility of the silica-supported metal oxide catalysts (■), *x*Mo and (□), *x*V.

led to the removal of approximately one oxygen atom per supported vanadium atom (Fig. 1), except for the highest loaded (3.0V) sample. The higher reducibility of dispersed vanadia compared with bulk V_2O_5 is consistent with previous reports (23, 35, 36). Temperature-programmed reduction (TPR) studies of vanadium oxide supported on alumina, titania, and silica show a decrease in the reducibility of vanadium oxide species with increasing coverage (37). Estimation of the dispersion of V_2O_5 on SiO_2 from TPR profiles has been accomplished using this characteristic (38).

MoO_3/SiO_2 catalysts of low loading (0.3–0.9 Mo/nm^2) show the same weight loss pattern as the V_2O_5/SiO_2 catalysts. The higher-loaded (1.3–3.5 Mo/nm^2) MoO_3/SiO_2 catalysts exhibited two distinct reduction stages: an initial rapid weight loss during the first few minutes (equivalent to that of the low-loaded samples) and then a slow process which reached equilibrium after approximately 3.5 h at 823 K. The appearance of the second reduction stage is associated with a decrease in the dispersion of molybdenum oxide species on silica, consistent with the appearance of surface polymolybdate species and crystalline orthorhombic molybdenum oxide features observed in Raman spectra of the dehydrated catalysts with concentrations of 1.3 Mo/nm^2 and above. This longer induction periods in isothermal reductions has been observed by Valyon *et al.* (39). Previous TPR studies (40) show that the longer time required to reduce the aggregated molybdenum oxide species appears to result in part to mass transfer limitations. In agreement with this, an experiment conducted with catalyst 1.3Mo using a H_2/He mixture showed a single reduction maximum. Kinetic limitation is responsible for the two-stage reduction observed in pure H_2 since no difference can be observed between dispersed and aggregated molybdenum oxide species in diluted hydrogen.

An increase in the reducibility of the higher-loaded SiO_2-supported molybdenum oxide catalysts is observed (Fig. 1) with respect to the lowest loaded sample, in the loading range characterized by dispersed surface molybdenum oxide species. Aggregation of the molybdenum oxide species results in a significant increase in the overall degree of reduction of the silica-supported molybdenum oxide species (Fig. 1) implying that the dispersed surface molybdenum oxide species are less reducible than the bulk molybdenum oxide species. Highly dispersed particles cannot be fully reduced as a minimum particle size is required for stabilization. Additionally, silanol groups are reported to oxidize isolated metal particles (41).

The increase in reducibility of molybdenum oxide species is indicative of some modification in the nature of molybdenum species. It may be related to the appearance of weak additional Raman features. As indicated by Raman spectroscopy, the amount of polymeric surface molybdenum oxide species is not very high, thus explaining the moderate increase in average reducibility of the silica-supported molybdenum oxide catalysts at molybdenum loadings below the onset of crystalline orthorhombic MoO_3 formation.

The relative weight loss measured in each stage can be used to evaluate the dispersion of silica-supported molybdenum oxide species since the two stages observed in the isothermal reduction of silica-supported molybdenum oxide catalysts can be related to the reduction of essentially dispersed (rapidly reduced) and bulk (slow reduction) molybdenum oxide phases. The percentage of dispersed molybdenum oxide estimated according to this method is presented in Fig. 2. It has previously been noted that the dispersed molybdenum oxide species show a Raman band at ca. 982 cm^{-1}. The evolution of the intensity of that Raman band with respect to the silica support band at 495 cm^{-1}, which is essentially constant, is indicative of the amount of dispersed surface molybdenum oxide species. Since at low molybdenum content most of the molybdenum is present as

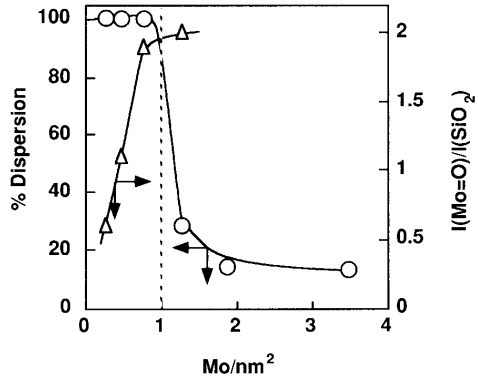

FIG. 2. Amount of dispersed surface mono-oxo-molybdenum oxide species estimated from I(Mo=O) at 982 cm^{-1} (△) versus the intensity of the silica band at 495 cm^{-1} and degree of dispersion of molybdenum oxide species estimated from the reduction measurements (○).

isolated surface molybdenum oxide species, this band provides a good estimation of the amount of dispersed surface molybdenum oxide species. These Raman intensities are included in Fig. 2. Initial increases in molybdenum loading results in an equivalent increase in the ratio of intensities at 982/495 cm^{-1}. The maximum in isolated molybdenum oxide species reached for a concentration of ca. 1.0 Mo/nm^2 indicated by the Raman signal corresponds with a silica surface in which very few available silanol groups remain (31, 42). For higher Mo concentrations, therefore, further formation of dispersed molybdenum oxide species is not expected. The appearance of additional Raman features and the intense Raman bands of crystalline orthorhombic MoO_3 for 1.9Mo and 3.5Mo support this assumption. Consequently, a significant decrease in the dispersion of the silica-supported molybdenum oxide species is expected. The dispersion estimations by the isothermal reduction experiments and the Raman spectroscopy show a good degree of correlation (Fig. 2). This estimation, however, cannot be made in a system where the bulk oxide is less reducible than the dispersed phase, as is the case for silica-supported vanadium oxide catalyst.

For both series, increasing the metal loading results in an increase in the initial reduction rate, (R_0) (Fig. 3). For the Mo/SiO_2 series, the sharp increase of initial reduction rate (R_0) in the low molybdenum loading region corresponds to the presence of incipient surface polymerization of molybdenum oxide species. With a further increase in size, as suggested by the improved definition of Raman bands due to polymeric surface molybdenum oxide species, the crystalline orthorhombic MoO_3 phase appears and a significant decrease in R_0 takes place. For V_2O_5/SiO_2 loadings above 1 V/nm^2, a less dramatic increase in R_0 with increasing loading is observed when compared with lower-loaded catalysts. At higher vanadium loadings (3.0 V/nm^2) the initial reduction rate declined significantly.

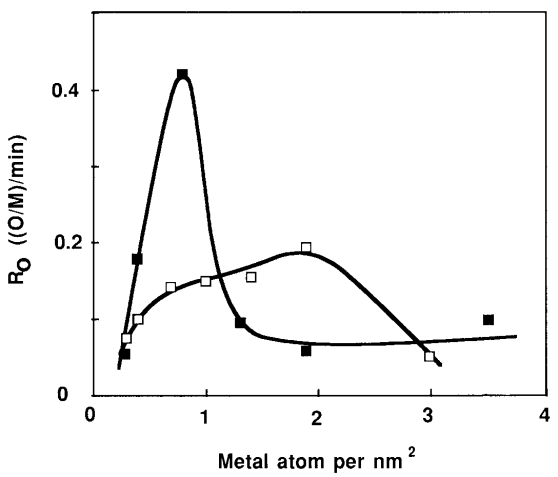

FIG. 3. Initial reduction rates (R_0) for xMo (■) and xV (□) series.

For supported vanadia catalysts, the change in slope observed between 0.8V and 1.8V corresponds with the formation of microcrystalline vanadium oxide, whereas the sharp decrease in R_0 above 2 V/nm^2 corresponds with the onset of formation of larger vanadium oxide crystallites.

The reduction of molybdenum oxide species has been shown to be highly dependent on its dispersion (40) and the initial rate of reduction for V_2O_5 crystals sensitive to the crystal thickness, according to the lattice parameter c (43). The reduction isotherms show that reduction occurs in two stages for the xMo series at concentrations above those showing a maximum in R_0. This reduction behavior is characteristic of bulk crystalline oxide (39). At 1.3 Mo/nm^2 molybdate species are formed while at higher loadings the formation of crystalline orthorhombic α-MoO_3 occurs. For the xV series the initial deviation of R_0 is associated with the onset of microcrystalline V_2O_5 species and the sharp decrease in R_0 corresponds with the onset of crystalline vanadium oxide formation.

Catalytic Activity

Prior to any measurement, the contribution of the gas-phase reaction was evaluated by performing a series of experiments with the empty reactor. The data obtained with the 8-mm-o.d. reactor and the results obtained in another series of experiments performed using an empty and SiC-filled 12-mm-o.d. reactor confirmed that the contribution of the gas-phase reaction in the temperature range studied is negligible, giving only trace amounts of dimerization products, mainly ethane, at temperatures above 873 K. Blank experiments were performed with the untreated support as formation of HCHO on several commercial silica substrates has been reported (15, 20). No significant activity would be expected as the Degussa Aerosil-200 used here is a fumed silica, prepared at high temperature. In the temperature range 823–953 K, for methane pseudo-contact time $W/F = 2.0$ g h/mol and $CH_4/O_2 = 10$ (molar ratio) in the feed, no HCHO was detected and carbon oxides and water were the major reaction products, with only trace amounts of ethane (dimerization) at the highest temperatures. The MoO_3/SiO_2 catalysts reached steady state according to GC analysis, whereas the V_2O_5/SiO_2 catalysts required ca. 4 h on stream to reach steady state.

The selective oxidation of methane on both the MoO_3/SiO_2 and V_2O_5/SiO_2 catalysts yielded essentially HCHO, CO, CO_2, and H_2O. Minor amounts of dimerization products and methanol were also observed. A reactor specifically designed to reduce the dead volume was used since the participation of the gas-phase reaction plays a significant role in further oxidizing the selective oxidation products (HCHO) (16). To understand the role played by the lattice oxygen of MoO_3 and V_2O_5 oxides in the selective oxidation of methane and to explain the relative reactivities of the two oxides, which provide basic insights into the

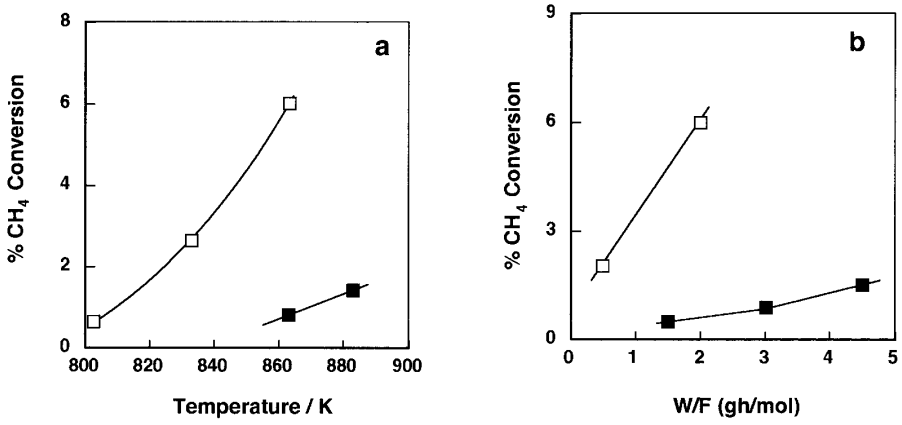

FIG. 4. Influence of (a) reaction temperature and (b) pseudo-residence time (W/F) on the conversion of methane for (□) 0.8V and (■) 0.8Mo. Reaction conditions: (a) $W/F = 2.0$ g h/mol; $CH_4/O_2 = 11$ M and (b) $T = 863$ K; $CH_4/O_2 = 11$ M.

reaction mechanism, a comparison of the catalytic behaviors in terms of: (i) methane conversion vs temperature, (ii) methane conversion vs contact time, and (iii) selectivity to HCHO vs conversion are described below. Activity and selectivity data obtained for a given set of experimental conditions were practically identical for repeated experiments.

The influence of the reaction temperature on methane conversion for two representative 0.8V and 0.8Mo samples (i.e., containing the same metal oxide surface concentration) is presented in Fig. 4a. An increase in reaction temperature results, as expected, in an increase in the methane and oxygen conversion. Figure 4b depicts the conversion of methane vs pseudo-residence time (W/F). Under any specific reaction condition V_2O_5/SiO_2 catalysts are significantly more reactive than MoO_3/SiO_2 catalysts. In fact, it is apparent that the onset reaction temperature for 0.8V is ca. 60 K less than that needed for 0.8Mo to obtain the same level of conversion. Similar observations have been reported by Spencer and Pereira (9) and Parmaliana *et al.* (15, 18).

Figure 5 shows the selectivity to HCHO, CO, and CO_2 vs methane conversion on the representative catalysts, 0.8V and 0.8Mo. The complementary selectivity trends between HCHO and CO strongly suggest that HCHO is further oxidized to CO for both MoO_3/SiO_2 and V_2O_5/SiO_2. However, the selectivity to CO_2 shows a different trend. CO_2 is formed at very low conversion on silica-supported molybdenum oxide catalysts and its selectivity does not appear to change significantly in the range of methane conversion studied. Conversely, for V_2O_5/SiO_2, no CO_2 is formed at very low methane conversion, but a further increase in CH_4 conversion results in an increase in formation of CO_2. It is apparent that carbon dioxide is a primary product for silica-supported molybdenum oxide catalysts whereas it would appear to be formed by further oxidation of CO on vanadia/silica catalysts. The reaction pathway for methane conversion initially proposed by Spencer and Pereira (9) has been verified by isotopic studies (22, 23, 28, 29). We have previously shown a simple means of demonstrating that CO_2 is a primary product on MoO_3/SiO_2 catalysts and that it can be enhanced by promoting secondary gas-phase

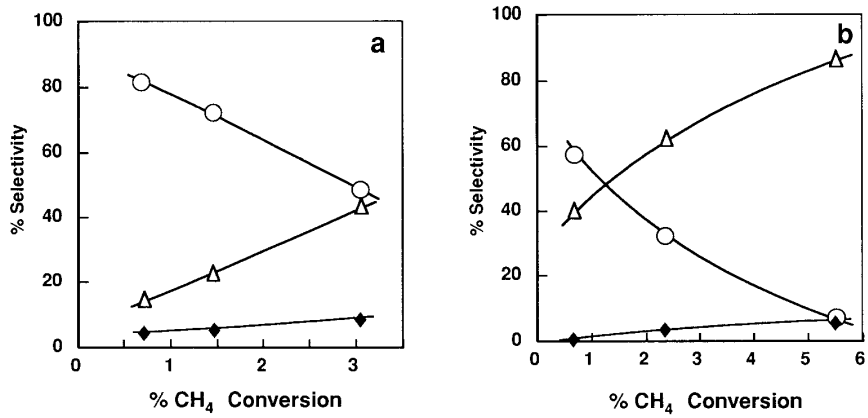

FIG. 5. Selectivity to HCHO (○); CO (△); and CO_2 (◆) vs CH_4 conversion for (a) 0.8Mo and (b) 0.8V.

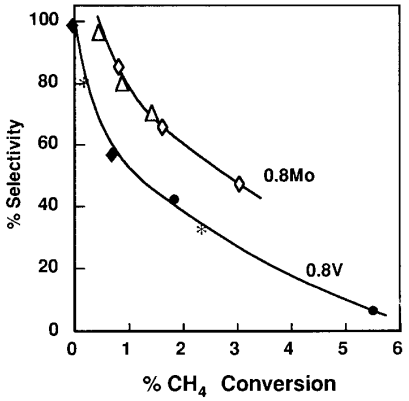

FIG. 6. Selectivity to HCHO on 0.8V and 0.8Mo vs methane conversion. (△) 0.8Mo at 863 K; (◇) 0.8Mo at 883 K; (◆) 0.8V at 803 K; (∗) 0.8V at 833 K; and (●) 0.8V at 863 K.

reactions (16). The activity of the 0.8Mo catalyst was measured using two reactors, one of which had a small dead volume downstream of the catalyst bed. Under the same reaction conditions, methane conversion was not altered although the product distribution was modified. An increase in residence time of the products in the hot zone (reactor with larger dead volume, 10-mm-o.d. reactor) decreased markedly the selectivity to HCHO with a corresponding increase to CO. The selectivity to carbon dioxide was only slightly affected. It would appear that HCHO and CO_2 are primary products in the oxidation of methane on silica-supported MoO_3 catalysts.

Figure 6 shows the selectivity to HCHO of 0.8V and 0.8Mo. The selectivity to HCHO is always lower for the silica-supported vanadium oxide catalysts. The differences observed between silica-supported molybdenum oxide and silica-supported vanadium oxide cannot be explained from the differences observed in their reducibility and initial reduction rates. In line with other studies on the selective oxidation of hydrocarbons, no definite correlation has been found between catalytic activity and catalyst reducibility (44, 45). We have already reported a similar absence of a link between catalyst reducibility and its activity in the selective conversion of methane (46). This trend is in contrast to behavior in methanol oxidation where hydrogen abstraction takes place and catalytic activity may be correlated with catalyst reducibility (46). In the case of methane oxidation, radicals are reported to be generated mainly in the gas phase and then converted on the supported metal oxide (20). Therefore, the main difference between both catalyst series must be related to their different capabilities to activate oxygen. Oxygen species transform upon adsorption on a metal oxide according to the following scheme (47):

$$O_2\,(\text{ads}) \rightarrow O_2^-\,(\text{ads}) \rightarrow O^-\,(\text{ads}) \rightarrow O^{2-}\,(\text{lattice}).$$

Predominant species should be determined by the nature of specific oxides. A continuous gradation of these species is expected to occur on the adsorption site. Molybdates are reported not to adsorb oxygen, in contrast to silica-supported vanadia (47). Isotopic studies show no oxygen exchange on silica-supported molybdenum oxide (22) and a small degree of oxygen exchange on silica-supported vanadium oxide (23, 29). This result leads us to assume a higher interaction of the silica-supported vanadium sites with gas-phase oxygen than in the case of silica-supported molybdenum oxide. Under catalytic reaction conditions interaction of both silica-supported oxides with methyl radicals results in the incorporation of lattice oxygen in the formaldehyde molecule, as indicated by isotopic studies on silica-supported molybdenum oxide (22, 28) and on silica-supported vanadium oxide (23, 29) during the selective oxidation of methane. For both systems oxygen vacancies are regenerated by gas-phase oxygen. In addition to surface lattice oxygen, adsorbed oxygen species (O_2^- and O^-) are also expected to be formed on silica-supported vanadium oxide catalysts (47). Ionic adsorbed oxygen species are reported to be more reactive and lead to nonselective oxidation, as in the case of methane combustion catalysts (48). Scarcity of adsorbed oxygen prevents lowering reaction selectivity (49). This may be the origin of the higher reactivity and lower selectivity of silica-supported vanadium oxide catalysts.

The methane turnover frequency (TOF) values are presented in Fig. 7 for the silica-supported metal oxide catalysts as a function of the surface metal coverage (metal atom/nm^2). The TOF values have been calculated under the assumption that all the supported metal is active. At low metal loadings (below 1.3 metal atom/nm^2) the TOF values remain essentially constant, except for 0.3V, which presents a remarkably low TOF. Similar profiles have been obtained

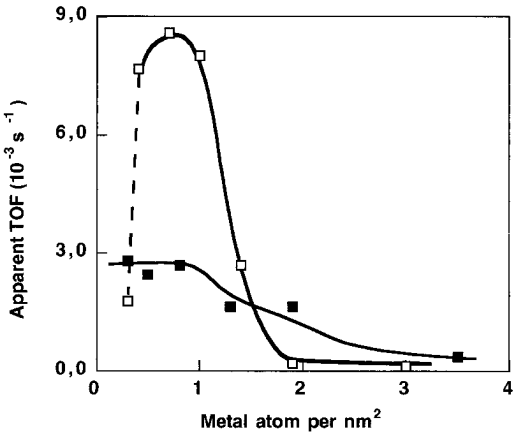

FIG. 7. Turnover frequency vs metal/nm^2 for Mo/SiO_2 (■) and V_2O_5/SiO_2. (□). Reaction conditions for MoO_3/SiO_2 863 K, $W/F = 3.0$ g h/mol and $CH_4/O_2 = 10$ M; for V_2O_5/SiO_2: 833 K, $W/F = 0.4$ g h/mol $CH_4/O_2 = 10$ M.

by Karthereuser *et al*. (29) using V_2O_5/SiO_2 catalysts for methane conversion. This loading range (<1 metal atom/nm^2) is characterized essentially by the existence of dispersed isolated surface metal (V or Mo) oxide species. The yield to partial oxidation products (HCHO) is less for V_2O_5/SiO_2 catalysts despite its higher reactivity (Fig. 6). The higher reactivity of the V_2O_5/SiO_2 series is essentially related to nonselective oxidation products. *In situ* Raman experiments during methane oxidation conditions show that supported vanadium oxide species undergo a slight reduction to lower oxidation states, thus providing oxygen adsorption sites (33). This reduction is not observed for MoO_3/SiO_2 catalysts (46). The reduced sites generated on V_2O_5/SiO_2 surfaces during methane oxidation, which act as adsorption sites to activate oxygen, appear to promote non-selective oxidation (33, 48). The high TOF number difference between the 0.3V sample and the other members of the series of low loadings is not clear. One possibility is that the very low conversion values do not allow a quantitative study of this specific catalyst. However, it is possible that, for very low loadings and consequently high dispersions where essentially all vanadium species exist as isolated entities, these species are incapable of providing both active oxygen and methane/methyl radical adsorption sites (e.g., H abstraction sites) and that this combination is only provided when nearest-neighbor vanadium species are present at higher loadings. At yet higher loadings, better-defined and larger crystals of V_2O_5 are present, decreasing the number of exposed vanadium sites, resulting in the dramatic drop in TOF. The TOF profile for MoO_3/SiO_2 is quite similar. Below the dispersion limit, the TOF number remains essentially constant and decreases for molybdenum loadings where crystalline MoO_3 species are present.

It appears that methane conversion on V_2O_5 materials is not only related to the surface vanadium species present but also to the partial reduction of these sites. These provide sites for nonselective oxidation products. During reaction under reducing conditions, the surface of the vanadium species undergoes a reduction that may be the origin of the induction period observed for V_2O_5/SiO_2, which was not detected for MoO_3/SiO_2 catalysts. Reactivity of MoO_3/SiO_2 catalysts is essentially linked to dispersed surface molybdenum oxide species and no surface reduction and consequently additional sources of reactivity are generated.

CONCLUSIONS

Characterization of the silica-supported molybdenum and vanadium oxides by laser Raman spectroscopy and reduction isotherms allows a critical surface metal loading to be determined above which supported metal oxide species are present as bulk oxide. Isolated dispersed metal oxide species are dominant on both catalyst series at lower metal loading. The higher reducibility of bulk-like molybdena vs surface molybdenum oxide species provides a simple means to evaluate dispersion of silica-supported molybdenum oxide.

Both supported V and Mo oxides are active in the conversion of methane to C_1-oxygenates and CO_x. Formaldehyde is a primary oxidation product, which is further oxidized to CO. The vanadium oxide catalysts are more reactive than the molybdenum oxide catalysts in conversion of methane; however, its higher reactivity also results in a further oxidation of HCHO to CO thus resulting in a lower yield to selective oxidation products.

Characterization and activity measurements indicate that surface dispersed metal oxide species are more reactive than aggregated metal oxide species.

ACKNOWLEDGMENTS

We thank the Spanish Ministry of Education and Science for financial support (M.A.B.). This work was partially supported by the Commission of the European Communities, EEC Contract JOU2-CT92-0040.

REFERENCES

1. Pitchai, R., and Klier, K., *Catal. Rev.-Sci. Eng.* **28**, 13 (1986).
2. Sinev, M. Yu., Korshak, V. N., and Krylov, O. V., *Russ. Chem. Rev.* **58**, 22 (1989).
3. Brown, J. J., and Parkyns, N. D., *Catal. Today* **8**, 305 (1991).
4. Khan, M. M., and Somorjai, G. A., *J. Catal.* **91**, 263 (1985).
5. Zhen, K. J., Khan, M. M., Mak, C. H., Lewis, K. B., and Somorjai, G. A., *J. Catal.* **94**, 501 (1985).
6. Kasztelan, S., and Moffat, J. B., *J. Catal.* **106**, 512 (1987).
7. Otsuka, K., and Hatano, M., *J. Catal.* **108**, 252 (1987).
8. Spencer, N. D., *J. Catal.* **109**, 187 (1988).
9. Spencer, N. D., and Pereira, C. J., *J. Catal.* **116**, 399 (1989).
10. Barbaux, Y., Elamrani, A. R., Payen, E., Gengembre, L., Grzybowska, B., and Bonnelle, J. P., *Appl. Catal.* **44**, 117 (1988).
11. Otsuka, K., Komatsu, T., Jinno, K., Uragami, Y., and Morikawa, K., *in* "Proceedings, 9th International Congress on Catalysis, Calgary 1988" (M. J. Phillips and M. Ternan, Eds.), Vol. 2, p. 915. Chem. Institute of Canada, Ottawa, 1988.
12. Kastanas, G. N., Tsigdinos, G. A., and Schwank, J., *Appl. Catal.* **44**, 33 (1988).
13. Amir-Ebrahimi, V., and Rooney, J. J., *J. Mol. Catal.* **50**, L17 (1989).
14. Mac Giolla Coda, E., Kennedy, M., McMonagle, J. B., and Hodnett, K. B., *Catal. Today* **6**, 559 (1990).
15. Parmaliana, A., Frusteri, F., Miceli, D., Mezzapica, A., Scurrell, M. S., and Giordano, N., *Appl. Catal.* **78**, L7 (1991).
16. Baldwin, T. R., Burch, R., Squire, G. D., and Tsang, S. C., *Appl. Catal.* **74**, 137 (1991).
17. Sojka, Z., Herman, R. G., and Klier, K., *J. Chem. Soc. Chem. Commun.* 185 (1991).
18. Miceli, D., Arena, F., Parmaliana, A., Scurrell, M. S., and Sokolovskii, V., *Catal. Lett.* **18**, 283 (1993).
19. Weng, T., and Wolf, E. E., *Appl. Catal. A* **96**, 383 (1993).
20. Sun, Q., Di Cosimo, J. I., Herman, R. G., Klier, K., Bhasin, M. M., *Catal. Lett.* **15**, 371 (1992).
21. Bañares, M. A., and Fierro, J. L. G., *in* "Catalytic Selective Oxidation" (S. T. Oyama and J. W. Hightower, Eds.), Chap. 21. Am. Chem. Soc., Washington, DC, 1993.

22. Bañares, M. A., Guerrero-Ruíz, A., Rodríguez-Ramos, I., and Fierro, J., *in* "New Frontiers in Catalysis" (L. Guczi, F. Solymosi, and P. Tétényi, Eds.), p. 1131, Elsevier, Amsterdam, 1993.
23. Koranne, M. J., Goodwin, J. G., and Marcelin, G., *J. Catal.* **148**, 378 (1994).
24. Koranne, M. J., Goodwin, J. G., and Marcelin, G., *J. Catal.* **148**, 388 (1994).
25. Hargreaves, S. J., Hutchings, G. J., and Joyner, R. W., *Nature* **348**, 428 (1992).
26. Bañares, M. A., Fierro, J. L. G., and Moffat, J. B., *J. Catal.* **142**, 406 (1993).
27. Bañares, M. A., and Fierro, J. L. G., *Catal. Lett.* **17**, 205 (1993).
28. Mauti, R., and Mims, C. A., *Catal. Lett.* **21**, 201 (1993).
29. Karthereuser, B., Hodnett, B. K., Zanthoff, H., and Baerns, M., *Catal. Lett.* **21**, 209 (1993).
30. Oyama, S. T., Went, G. T., Lewis, K. B., Bell, A. T., and Somorjai, G. A., *J. Phys. Chem.* **93**, 6786 (1989).
31. Roark, R. D., Kohler, S. D., Ekerdt, J. G., Kim, D. S., and Wachs, I. E., *Catal. Lett.* **16**, 77 (1993).
32. Williams, C. C., Ekerdt, J. G., Jehng, J-.M., Hardcastle, F. D., Turek, A. M., and Wachs, I. E., *J. Phys. Chem.* **95**, 8781 (1991).
33. Sun, Q., Jehng, J.-M., Hu, H., Herman, R. G., Wachs, I. E., and Klier, K., *in* "Symposium on Methane and Alkane Activation, San Diego, March 13–18, 1994" Am. Chem. Soc., Washington, DC.
34. Das, N., Ekerdt, H., Hu, H., Wachs, I. E., Walzer, J. F., and Feher, F. J., *J. Phys. Chem.* **97**, 8240 (1993).
35. Wachs, I. E., Saleh, R. Y., Chan, S. S., and Chersich, C. C., *Appl. Catal.* **15**, 339 (1985).
36. Haber, J., Kozłowska, A., and Kozłowski, R., *J. Catal.* **102**, 52 (1986).
37. Roozeboom, F., Mittlemaijer-Hazeleger, M. C., Moulijn, J. A., Medema, J., de Beer, V. H. J., and Gellings, P. J., *J. Chem. Phys.* **84**, 2783 (1980).
38. Koranne, M. J., Goodwin, J. G., and Marcelin, G., *J. Catal.* **148**, 369 (1994).
39. Valyon, J., Henker, M., and Wendandt, K.-P., *React. Kinet. Catal. Lett.* **38**, 265 (1989).
40. Regalbuto, J. R., and Ha J.-W., *Catal. Lett.* **29**, 189 (1994).
41. Howe, R. F., *in* "Tailored Metal Catalysts" (Y. Iwasawa, Ed.), Reidel, Dordrecht, 1986.
42. Liu, T.-Ch., Forissier, M., Coudurier, G., and Védrine, J. C., *J. Chem. Soc. Faraday Trans. 1* **85**, 1607 (1989).
43. Tilley, R. J. D., and Hyde, B. G., *J. Phys. Chem. Solids* **31**, 613 (1970).
44. Moro-Oka, Y., Morikawa, Y., and Ozaki, A., *J. Catal.* **7**, 23 (1967).
45. Oyama, S. T., Desikan, A. N., and Zhang, W., *in* "Catalytic Selective Oxidation" (S. T. Oyama and J. W. Hightower, Eds.), Chap. 2. Am. Chem. Soc., Washington DC, 1993.
46. Bañares, M. A., Jones, M. D., Spencer, N. D., and Wachs, I. E., *J. Catal.* **146**, 204 (1994).
47. Bielanski, A., and Haber, J., *Catal. Rev.-Sci. Eng.* **19**, 1 (1979).
48. Seiyama, T., *in* "Properties and Applications of Perovskite-Type Oxides" (L. G. Tejuca and J. L. G. Fierro, Eds.), Chap. 10. Dekker, New York, 1993.
49. Fierro, J. L. G., *in* "Spectroscopic Characterization of Heterogeneous Catalysts, Part B: Chemisorption of Probe Molecules" (J. L. G. Fierro, Ed.). Elsevier, Amsterdam, 1990.